Theoretical infrared spectra of large polycyclic aromatic hydrocarbons

Amit Pathak, Shantanu Rastogi *

Department of Physics, D.D.U. Gorakhpur University, Gorakhpur 273 009, India

Abstract

Theoretical and experimental spectroscopic studies have underlined the contribution of large PAHs towards the astrophysical mid-infrared emission bands. Quantum chemical study of eight large PAHs using density functional theory approach is reported along with their infrared spectra. Systematic variation of bands with PAH size is noted and a better agreement with the observed astrophysical bands is obtained. Compared to small and medium sized PAHs there is substantial $C-H$ stretch intensity in the cation spectra. This is attributed to smaller change in charge on the hydrogens upon ionization. For the $C-H$ out-of-plane mode large PAHs correlate well with observed features on the shorter wavelength side of the 11.2 μm band. Presence of two sub-components of the broad 7.7 μm band in large PAHs compares very well with the corresponding astrophysical band and point to the abundance of large PAH cations in interstellar environments. The data presented here may be used for a more detailed study on the profile variations accompanying the mid-IR bands in various interstellar environments.

Key words: PAH, Interstellar molecules, DFT, IR spectra, Aromatic Infrared Bands

1 Introduction

The mid-Infrared (IR) spectra of a variety of astrophysical sources is dominated by emission features at 3030, 1610, 1310, 1160 and 890 cm^{-1} (3.3, 6.2, 7.7, 8.6 and 11.2 μm) commonly known as the aromatic infrared bands (AIBs). These features have been observed in the spectra of star forming regions, HII regions, reflection nebulae, planetary nebulae, young stellar objects (YSO) and

* Corresponding author
Email address: shantanu_r@hotmail.com (Shantanu Rastogi).

galaxies [1–8]. Polycyclic Aromatic Hydrocarbons (PAHs) are widely accepted to be the carriers of these mid-IR emission bands [9–13]. The AIBs arise out of collective emission from a complex mixture of PAHs [13]. This mixture may comprise neutral PAHs, PAH cations, hydrogenated/de-hydrogenated as well as substituted PAHs. The nature of emitting condition decides the components of the mixture with more neutrals and hydrogenated ones in benign conditions as in proto planetary nebula and cations and de-hydrogenated ones in UV rich environments as in HII regions, reflection nebulae, etc. [13].

Emission mechanism of PAHs involves vibrational heating of a PAH molecule up to a temperature of 1000 K by the absorption of a single UV photon. The excited PAH molecule then undergoes internal vibrational redistribution to distribute the absorbed energy over different vibrational modes. The molecule de-excites through IR fluorescence [11,12] resulting in mid-IR emissions. Recent studies show that the excitation of a PAH molecule may also be due to longer wavelength photons, i.e., visible and near IR photons [14–17]. This accounts for the observations of AIBs in UV-poor objects [5,18].

Extrapolating the spacing between 6.2 and 7.7 μm feature, Hudgins and Allamandola [19] have concluded that PAHs with 50–80 carbon atoms dominate the mid-IR emission. A similar conclusion has been derived from studies testing the photo-physical stability of PAHs [20–23]. Large PAHs are quite stable and are the most viable candidates to be present in the inter-stellar medium (ISM). Laboratory synthesis of large PAHs (> 50 carbon atoms) is extremely difficult and so is the experimental measurement of the spectra. Calculations using density functional theory (DFT) play a vital role to provide the IR information of such species for comparison with observations [24–29]. Fair amount of experimental [30–39] and theoretical [24–28] studies have been done to understand the IR spectra of PAHs that show the accuracy of DFT method and its use to complement the experimental spectra. The DFT results are also being used as inputs for theoretical emission models [40–44] which are useful for direct matching with the AIB emissions. In this communication we report the IR spectra of eight large PAHs and study the variations of bands with PAH size. The results are discussed in the context of AIBs and may prove useful for understanding the interstellar spectra and its variations in diverse interstellar conditions.

GAMESS ab-initio program [45] is used for calculations under DFT using B3LYP functionals along with 4-31G basis expansion. The use of 4-31G basis set for calculations on PAHs is well established and a single scale factor suffices to bring the vibrational frequencies in conjunction with the experimental data [24,27–29]. The drawback associated with 4-31G basis is the overestimation of the $C-H$ stretch intensity. The use of larger basis sets 6-31G or 6-31G**, give comparatively better orbital representation and consequently a better $C-H$ stretch intensity match with experiments [24,27,29]. But the computational

effort increases many–folds and the scaling procedure also gets complicated [46,47]. Therefore, the use of larger basis sets is avoided. Comparison with experimental data wherever available shows that the $C-H$ stretch intensity is overestimated by about 1.4 to 2.0 times [24,27,28]. In the absence of experimental data the correction for the intensity overestimation is not possible. The intensity correction becomes important only for the study of relative intensity correlation of 3.3 μm AIB with other AIBs.

The calculated frequencies for some smaller PAHs – naphthalene, anthracene and pyrene, were compared with the reported matrix isolation spectra to obtain the best fit scale factor of 0.956. The frequencies of all studied PAHs [27,28] are scaled by this single factor. Only the most intense modes have been presented in the tables whereas all the modes have been considered for plotting the spectra of the studied PAHs. The theoretical spectra have been plotted considering Gaussian profiles with Full Width Half Maximum to be 30 cm^{-1}, which is the typical width for PAHs emitting in conditions present in the ISM [12]. Several modes closer than this collect together resulting in a single broad peak which may be shifted from the corresponding value given in the table.

Calculation time for symmetric PAHs is much less compared to lower symmetry PAHs of similar dimension. So mostly symmetric PAHs have been chosen in this study (Fig. 1). The eight studied PAHs are $C_{38}H_{16}$, $C_{48}H_{18}$, $C_{62}H_{20}$ (circum-bisanthene), $C_{66}H_{20}$ (circum-ovalene), $C_{80}H_{22}$, $C_{90}H_{24}$, $C_{96}H_{24}$ (circum-circum-coronene) and $C_{57}H_{19}$. All these PAHs have D_{2h} symmetry except for $C_{38}H_{16}$ which has C_{2h} symmetry and $C_{57}H_{19}$ which is totally asymmetric. $C_{96}H_{24}$ has D_{6h} symmetry in the neutral state and D_{2h} symmetry in the cationic state. Large PAHs may form as a result of defragmentation of carbonaceous composites which may be with lower or no symmetry. The asymmetric PAH in the sample offers opportunity to explore the effect of symmetry on the IR spectra of PAHs.

Optimized geometry and charge distribution of each species, in neutral and cationic forms, is calculated followed by the IR spectra at the optimized geometry. The results at this level of calculation are being presented for the first time except for $C_{96}H_{24}$ [26]. The chosen sample allows study of variations in the IR spectra with gradually increasing PAH size. These variations are underlined and their astrophysical relevance with reference to the profile variations of AIBs is discussed.

2 Results

The spectra of neutral PAHs are dominated by $C-H$ stretch and $C-H$ out of plane bend modes, whereas in cations the intensity of $C-H$ in plane bend and $C-C$ stretch modes (1150–1600 cm^{-1}) are increased by an order of magnitude and the $C-H$ stretch mode intensity is reduced [24,27,48]. Small variation is present in the intensity of $C-H$ out of plane bend mode but significant shift in band position is noted.

To understand the changes in the IR spectra upon ionization of PAHs the corresponding structural and charge changes are noted. Upon ionization there are negligible structural changes as also seen in smaller PAHs [27,28,49]. For highly symmetric $C_{96}H_{24}$, the point group symmetry is lowered from D_{6h} in neutral to D_{2h} in the cation. It seems that upon ionization of such highly symmetric species, the π orbitals mix to localize on one side of the molecule, resulting in reduction of symmetry [50]. This is a consequence of Jahn-Teller effect wherein the degenerate orbitals of highly symmetric species are split to lower the symmetry of ionized molecules [51]. Such lowering of symmetry is also seen for triphenylene and coronene cations [28]. A similar symmetry lowering, attributed to Jahn-Teller effect, is reported for coronene mono-anion [52].

Charge distributions for smaller PAHs have already been discussed [27,28]. It has been noted that the charge on the innermost carbon atoms is small in all the neutral species and minor change is present upon ionization. Similar charge variation is present for large PAHs. In neutrals the outer carbons carry negative charge and the hydrogens are positively charged. Significant change in charges of these atoms is noticed upon ionization. These charge changes affect the intensities of various modes particularly the $C-H$ stretch vibrations and the $C-C$ stretch modes[27,28].

The calculated spectra of each studied PAH is presented and discussed briefly. The vibrational frequencies and corresponding intensities along with irreducible representations have also been provided for intense modes. The complete IR data may be obtained from the authors upon request.

The spectra of $C_{38}H_{16}$ and $C_{48}H_{18}$ are displayed in Fig. 2. Vibrational frequencies and intensities of these molecules are tabulated in Tables 1 and 2. The spectrum of neutral $C_{38}H_{16}$ is dominated by the features due to out-of-plane $C-H$ vibrations (907 cm^{-1}) and $C-H$ stretch vibrations (3082 cm^{-1}). Apart from these, features at 763 and 1575 cm^{-1} are also quite intense. $C_{38}H_{16}$ has a couple of duo and trio along with six solo hydrogen atoms so the out-of-plane solo mode (907 cm^{-1}) is more intense than the duo-trio mode (763 cm^{-1}). For smaller PAHs where the number of duo-trio-quartet are more than solo hy-

drogens the intensity of 740-830 cm^{-1} feature is more than the 890-920 cm^{-1} feature [27,28,53]. The spectrum of $C_{38}H_{16}$ cation has several intense peaks. Features at 927, 1215, 1305, 1533, 1559 and 1591 cm^{-1} are of comparable intensity (Table 1). The $C-C$ stretch peak at 1305 cm^{-1} is due to overlap of less intense features which are less than 30 cm^{-1} apart and appear as the most intense band. But the absolute intensity of the $C-H$ out-of-plane bend vibration at 927 cm^{-1} is maximum. The feature due to $C-H$ stretch vibrations is also having significant intensity.

In $C_{48}H_{18}$ the out-of-plane vibration of solo hydrogen atoms result in an intense peak at 915 cm^{-1} and $C-H$ stretch vibration produce a peak at 3079 cm^{-1}. Eight solo hydrogen atoms contribute to the intensity of the band at 915 cm^{-1} while a couple of duo and trio hydrogens produce weak bands at 799 and 762 cm^{-1} respectively. Feature at 1539 cm^{-1} is of moderate intensity while less intense features close to 1375 and 1459 cm^{-1} are also present in the spectrum of the neutral molecule (Table 2). In the spectrum of cation overlap of several modes result in the most intense peak at 1529 cm^{-1}. The $C-H$ solo out-of-plane bend vibration and $C-C$ stretch vibrations result in almost equal intensity peaks at 931 and 1305 cm^{-1}. The $C-H$ stretch peak also shows up in the cation spectra. Feature due to the out-of-plane vibrations of hydrogen atoms is having significant intensity in the spectra of both $C_{38}H_{16}$ and $C_{48}H_{18}$ cations.

Spectra of *circum-bisanthene* ($C_{62}H_{20}$) and *circum-ovalene* ($C_{66}H_{20}$) are shown in Fig. 3. Table 3 gives the frequencies and intensities for $C_{62}H_{20}$ neutral and cation. The spectrum of neutral $C_{62}H_{20}$ has two distinct peaks due to out-of-plane vibrations of hydrogen atoms. The peak at 913 cm^{-1} is due to the wag of solo hydrogen atoms but the spectra is dominated by the feature at 844 cm^{-1} resulting from the out-of-plane vibrations of duo hydrogen atoms. The $C-C$ stretch vibrations produce a feature at 1590 cm^{-1} of significant intensity. Spectrum of the cation is simple in comparison to the spectra of $C_{38}H_{16}$ and $C_{48}H_{18}$ cations. The most intense peak in the spectrum of cation is at 1285 cm^{-1}. The feature near 1230 cm^{-1} is of comparable intensity. The $C-C$ stretch mode produces an intense feature at 1565 cm^{-1} which is nearly equal in intensity to the features arising out of $C-H$ stretch and out-of-plane bend vibrations.

The frequencies and relative intensities for neutral *circum-ovalene* are tabulated in Table 4. Spectrum of neutral $C_{66}H_{20}$ (Fig. 3) comprises mainly of two very intense peaks at 917 and 3055 cm^{-1}. Out-of-plane vibrations of the six pairs of duo hydrogens result in a small peak at 796 cm^{-1} (Table 4). Spectrum of the cation has intense peaks for $C-H$ in-plane and $C-C$ stretch vibrations at 1215 and 1314 and 1563 cm^{-1} respectively. The $C-C$ stretch peak at 1563 cm^{-1} is of highest intensity while the intensity of the feature due to $C-H$ in-plane vibrations at 1215 cm^{-1} is comparable to the intensity of

Table 1
Computed IR Frequencies (cm^{-1}) and Relative Intensities for $C_{38}H_{16}$

Neutral			Cation		
	Freq (cm^{-1})	Rel. Int.		Freq (cm^{-1})	Rel. Int.
A_u	763.4	0.46	B_u	535.0	0.08
A_u	788.3	0.09	A_u	611.5	0.06
A_u	907.4	0.62	B_u	644.3	0.06
A_u	910.4	0.20	A_u	711.1	0.07
B_u	1206.1	0.05	A_u	759.1	0.16
B_u	1253.8	0.08	A_u	770.7	0.11
B_u	1443.9	0.06	A_u	794.9	0.23
B_u	1470.6	0.08	B_u	817.1	0.06
B_u	1533.3	0.09	A_u	897.7	0.07
B_u	1554.4	0.05	A_u	921.1	0.05
B_u	1575.2	0.19	A_u	926.7	1.00
B_u	3038.1	0.06	B_u	1186.8	0.07
B_u	3041.8	0.23	B_u	1200.3	0.11
B_u	3056.7	0.22	B_u	1215.1	0.98
B_u	3061.8	0.17	B_u	1256.1	0.22
B_u	3065.4	0.56	B_u	1288.7	0.81
B_u	3081.7	1.00	B_u	1300.0	0.39
			B_u	1321.4	0.91
			B_u	1336.4	0.08
			B_u	1340.9	0.53
			B_u	1374.6	0.12
			B_u	1439.7	0.14
			B_u	1470.2	0.42
			B_u	1500.4	0.14
			B_u	1523.1	0.39
			B_u	1533.3	0.82
			B_u	1558.7	0.72
			B_u	1591.1	0.98
			B_u	3080.4	0.08
			B_u	3082.2	0.27
			B_u	3101.5	0.38

Max. absolute int. Neutral - 4.85 Debye^2/AMU-Å^2 (204.94 Km/mole); Cation - 3.51 Debye^2/AMU-Å^2 (148.32 Km/mole)

Table 2
Computed IR Frequencies (cm^{-1}) and Relative Intensities for $C_{48}H_{18}$

Neutral			Cation		
	Freq (cm^{-1})	Rel. Int.		Freq (cm^{-1})	Rel. Int.
B_{1u}	373.8	0.05	B_{1u}	373.4	0.07
B_{3u}	617.1	0.04	B_{2u}	618.3	0.09
B_{3u}	762.6	0.13	B_{3u}	648.5	0.05
B_{3u}	799.3	0.15	B_{3u}	769.3	0.15
B_{1u}	819.0	0.08	B_{3u}	806.4	0.26
B_{3u}	909.6	0.05	B_{1u}	819.3	0.17
B_{3u}	915.5	0.69	B_{1u}	931.0	0.09
B_{1u}	1222.4	0.06	B_{3u}	931.2	0.99
B_{1u}	1375.4	0.15	B_{1u}	1127.3	0.16
B_{1u}	1459.2	0.13	B_{1u}	1169.9	0.07
B_{1u}	1538.9	0.23	B_{2u}	1192.5	0.37
B_{1u}	1575.3	0.05	B_{2u}	1220.8	0.45
B_{1u}	1598.5	0.05	B_{2u}	1278.9	0.31
B_{2u}	3049.9	0.30	B_{2u}	1292.7	0.89
B_{2u}	3053.0	0.25	B_{2u}	1321.9	0.61
B_{2u}	3057.2	0.12	B_{1u}	1339.9	0.19
B_{2u}	3067.2	0.41	B_{2u}	1381.1	0.19
B_{1u}	3079.3	1.00	B_{1u}	1381.7	0.27
			B_{1u}	1394.5	0.07
			B_{1u}	1461.3	0.25
			B_{2u}	1479.8	0.34
			B_{2u}	1528.9	1.00
			B_{1u}	1532.3	0.39
			B_{2u}	1540.9	0.95
			B_{1u}	1555.7	0.78
			B_{2u}	1597.9	0.44
			B_{2u}	3080.8	0.31
			B_{1u}	3099.0	0.57

Max. absolute int. Neutral - 6.82 Debye^2/AMU-Å^2 (288.18 Km/mole); Cation - 4.53 Debye^2/AMU-Å^2 (191.42 Km/mole)

Table 3
Computed IR Frequencies (cm^{-1}) and Relative Intensities for $C_{62}H_{20}$

Neutral			Cation		
	Freq (cm^{-1})	Rel. Int.		Freq (cm^{-1})	Rel. Int.
B_{3u}	560.5	0.05	B_{3u}	852.9	0.61
B_{2u}	600.7	0.07	B_{3u}	932.9	0.33
B_{3u}	844.4	0.99	B_{1u}	1206.3	0.05
B_{3u}	913.3	0.71	B_{2u}	1217.4	0.23
B_{2u}	1066.6	0.11	B_{1u}	1226.1	0.64
B_{2u}	1142.9	0.06	B_{1u}	1247.7	0.44
B_{1u}	1247.4	0.05	B_{2u}	1268.9	0.09
B_{2u}	1261.4	0.06	B_{1u}	1285.0	1.00
B_{2u}	1268.1	0.08	B_{1u}	1295.3	0.06
B_{1u}	1275.2	0.07	B_{2u}	1325.9	0.36
B_{2u}	1322.9	0.09	B_{1u}	1334.3	0.09
B_{1u}	1327.5	0.06	B_{2u}	1445.3	0.09
B_{1u}	1362.4	0.06	B_{2u}	1458.1	0.15
B_{2u}	1442.1	0.06	B_{1u}	1509.4	0.10
B_{2u}	1520.6	0.14	B_{2u}	1530.4	0.16
B_{1u}	1581.1	0.26	B_{2u}	1552.5	0.07
B_{2u}	1602.9	0.26	B_{2u}	1564.6	0.49
B_{2u}	3020.5	0.48	B_{1u}	1568.7	0.16
B_{2u}	3030.4	0.58	B_{2u}	1591.2	0.23
B_{1u}	3031.4	0.69	B_{1u}	1593.9	0.11
B_{2u}	3068.5	1.00	B_{2u}	3081.9	0.26
B_{1u}	3081.8	0.69	B_{1u}	3092.6	0.26

Max. absolute int. Neutral - 4.13 Debye^2/AMU-Å^2 (174.51 Km/mole); Cation - 7.56 Debye^2/AMU-Å^2 (319.45 Km/mole)

$C-C$ stretch peak at 1314 cm^{-1}. Significant intensity is present in features due to $C-H$ vibrations, i.e., $C-H$ solo wag at 934 cm^{-1} and $C-H$ stretch vibrations at 3068 cm^{-1}.

The spectra of $C_{80}H_{22}$ and $C_{90}H_{24}$ are shown in Fig. 4. Table 5 and 6 give the frequencies and intensities of these PAHs. Spectrum of the neutral $C_{80}H_{22}$ has two intense peaks involving $C-H$ vibrations at 3072 cm^{-1} (stretch) and 920 cm^{-1} (solo out-of-plane bend). The out-of-plane vibrations of duo hydrogen atoms result in a small peak at 803 cm^{-1}. The $C-C$ stretch vibrations produce

Table 4
Computed IR Frequencies (cm^{-1}) and Relative Intensities for $C_{66}H_{20}$

Neutral			Cation		
	Freq (cm^{-1})	Rel. Int.		Freq (cm^{-1})	Rel. Int.
B_{1u}	599.5	0.07	B_{3u}	802.3	0.13
B_{3u}	796.0	0.28	B_{3u}	918.7	0.13
B_{3u}	904.8	0.20	B_{3u}	934.0	0.34
B_{3u}	917.3	1.00	B_{1u}	1127.5	0.05
B_{2u}	1159.0	0.07	B_{2u}	1211.0	0.31
B_{1u}	1215.2	0.06	B_{1u}	1215.4	0.44
B_{1u}	1219.1	0.09	B_{2u}	1238.0	0.07
B_{2u}	1261.1	0.13	B_{1u}	1267.4	0.38
B_{1u}	1365.5	0.08	B_{2u}	1269.1	0.07
B_{1u}	1581.2	0.16	B_{1u}	1299.1	0.53
B_{2u}	1582.3	0.08	B_{2u}	1306.9	0.13
B_{2u}	1598.1	0.08	B_{1u}	1318.7	0.08
B_{1u}	1604.9	0.07	B_{2u}	1328.0	0.37
B_{2u}	3019.2	0.46	B_{2u}	1362.0	0.08
B_{1u}	3026.6	0.23	B_{2u}	1455.2	0.27
B_{1u}	3029.4	0.36	B_{2u}	1498.8	0.14
B_{2u}	3029.5	0.29	B_{2u}	1535.5	0.33
B_{1u}	3043.9	0.84	B_{2u}	1543.9	0.06
B_{1u}	3067.0	0.31	B_{2u}	1563.4	1.00
B_{2u}	3067.1	0.86	B_{1u}	1568.7	0.12
			B_{1u}	1597.9	0.13
			B_{1u}	3056.8	0.19
			B_{2u}	3080.0	0.18

Max. absolute int. Neutral - 4.96 Debye^2/AMU-Å^2 (209.59 Km/mole); Cation - 12.35 Debye^2/AMU-Å^2 (521.85 Km/mole)

a band centred at 1580 cm^{-1}. Spectrum of the cation has a very intense peak at 1566 cm^{-1} due to $C-C$ stretch vibrations. Intensity of all other features is similar and nearly half of the most intense peak. The $C-H$ stretch feature at 3084 cm^{-1} and $C-C$ stretch and $C-H$ in-plane bend features at 1295 and 1217 cm^{-1} respectively are of significant intensity. $C-H$ out-of-plane bend feature results in a small peak in the cation spectra.

The spectrum of neutral $C_{90}H_{24}$ (Fig. 4) is similar to other PAHs having two

Table 5
Computed IR Frequencies (cm^{-1}) and Relative Intensities for $C_{80}H_{22}$

Neutral			Cation		
	Freq (cm^{-1})	Rel. Int.		Freq (cm^{-1})	Rel. Int.
B_{3u}	803.2	0.20	B_{3u}	810.1	0.08
B_{2u}	903.0	0.07	B_{3u}	934.2	0.29
B_{3u}	919.6	0.85	B_{2u}	1119.2	0.06
B_{2u}	1193.0	0.11	B_{2u}	1144.5	0.07
B_{1u}	1267.9	0.08	B_{2u}	1175.6	0.07
B_{1u}	1371.5	0.05	B_{1u}	1194.2	0.11
B_{2u}	1375.3	0.05	B_{2u}	1216.9	0.49
B_{1u}	1566.2	0.08	B_{1u}	1230.5	0.06
B_{2u}	1578.5	0.09	B_{2u}	1280.2	0.36
B_{1u}	1580.2	0.08	B_{2u}	1294.8	0.34
B_{1u}	1602.7	0.08	B_{1u}	1312.5	0.09
B_{2u}	3017.9	0.29	B_{2u}	1316.2	0.12
B_{2u}	3050.8	0.05	B_{2u}	1352.8	0.10
B_{2u}	3052.8	0.49	B_{2u}	1372.1	0.17
B_{1u}	3052.9	0.12	B_{1u}	1456.9	0.97
B_{2u}	3068.9	0.54	B_{2u}	1510.1	0.41
B_{2u}	3071.6	0.23	B_{2u}	1540.8	0.22
B_{1u}	3072.0	1.00	B_{2u}	1566.2	1.00
			B_{2u}	1592.2	0.32
			B_{1u}	1596.3	0.05
			B_{2u}	3063.5	0.13
			B_{2u}	3080.1	0.13
			B_{1u}	3083.8	0.22

Max. absolute int. Neutral - 7.26 Debye^2/AMU-Å^2 (306.77 Km/mole); Cation -19.52 Debye^2/AMU-Å^2 (824.82 Km/mole)

very intense peaks at 917 and 3030 cm^{-1} resulting from solo hydrogen wag and $C-H$ stretch vibrations. The out-of-plane vibrations of duo hydrogen atoms give rise to a small peak at 793 cm^{-1} (Table 6). The peak at 1567 cm^{-1} due to $C-C$ stretch vibrations is quite intense in the spectrum of neutral $C_{90}H_{24}$. In the spectra of $C_{90}H_{24}$ cation, two peaks at 1217 and 1284 cm^{-1} arising out of $C-H$ in-plane and $C-C$ stretch vibrations respectively stand out amongst all the modes. The band around 1600 cm^{-1} is usually a very high intensity band in the spectra of PAH cations, but in the spectra of $C_{90}H_{24}$

cation the intensity of this mode is even less than the $C-H$ out-of-plane and $C-H$ stretch features. This makes the spectrum of $C_{90}H_{24}$ cation different from other cations. Analysis shows that only a few $C-C$ bonds in the outer rings having duo hydrogens participate and give rise to this small peak while carbons constituting the rings having solo hydrogens show no motion at all. Addition of several $C-H$ stretch features produces a broad peak at 3042 cm^{-1}.

Spectra of $C_{96}H_{24}$ (Circum-circum-coronene) is given in Fig. 5. The frequencies and intensities for this PAH have been reported earlier [26]. Comparison with the earlier theoretical spectra (see Tables 7 and 8) shows a reasonably good match for both the neutral and cation except for the feature at 922 cm^{-1} (spectra of neutral) that does not match the intensity of the similar feature reported earlier [26]. In the absence of any reported experimental spectra these data are predictive. The spectrum of neutral molecule has two intense peaks at 921 cm^{-1} due to out-of-plane vibrations of solo hydrogen atoms and at 3031 cm^{-1} due to $C-H$ stretch vibrations. Out-of-plane vibrations of duo hydrogens result in a small peak at 808 cm^{-1}. Peaks nearly equal in intensity to this one are at 1160 cm^{-1} due to $C-H$ in plane vibrations, 1260 cm^{-1} and 1576 cm^{-1} due to $C-C$ stretch vibrations. In the spectra of cation the $C-H$ in plane vibrations at 1204 cm^{-1} and $C-C$ stretch vibrations at 1559 and 1316 cm^{-1} are most intense. The $C-H$ stretch mode at 3083 cm^{-1} also has significant intensity.

Calculations for a non-symmetrical molecule $C_{57}H_{19}$ have been done in order to see the effect of symmetry on the IR spectra of PAHs. The neutral and cation spectra are shown in Fig. 5. and the frequencies and intensities are tabulated in Table 9. Neutral $C_{57}H_{19}$ has an open shell configuration while the cation is a closed shell specie. Theoretical calculations on closed shell PAH cations have been reported and discussed earlier [54]. The most intense peak in the spectrum of neutral is at 901 cm^{-1} due to $C-H$ out-of-plane vibrations of solo hydrogen atoms. Out-of-plane vibrations of duo hydrogens produce a peak at 833 cm^{-1} of significant intensity. The asymmetrical nature of the molecule results in several modes for the $C-H$ stretch vibrations which overlap in to a broad and high intensity peak near 3068 cm^{-1}. Spectrum of the cation is similar to other studied PAHs. $C-C$ stretch vibrations produce intense peaks at 1569 and 1309 cm^{-1}. The peak at 1216 cm^{-1} is a result of $C-H$ in-plane vibrations. The $C-H$ stretch and $C-H$ out-of-plane modes have small intensity. Except for several modes being active to result in broad peaks (for e.g. the $C-H$ stretch modes in the neutral spectra), no dramatic changes originate due to asymmetry. Symmetric PAHs are more stable and more likely in the ISM. Asymmetric PAHs formed from defragmentation of grains may be short lived unless they are compact and somehow rendered stable.

Table 6
Computed IR Frequencies (cm^{-1}) and Relative Intensities for $C_{90}H_{24}$

Neutral			Cation		
	Freq (cm^{-1})	Rel. Int.		Freq (cm^{-1})	Rel. Int.
B_{1u}	274.6	0.06	B_{3u}	799.4	0.07
B_{3u}	793.2	0.23	B_{3u}	919.7	0.14
B_{2u}	794.2	0.07	B_{3u}	935.9	0.22
B_{3u}	907.6	0.33	B_{1u}	1106.7	0.06
B_{3u}	919.9	1.00	B_{2u}	1206.7	0.15
B_{2u}	959.6	0.06	B_{1u}	1218.4	0.60
B_{2u}	1156.1	0.09	B_{1u}	1257.5	0.15
B_{1u}	1233.5	0.14	B_{1u}	1271.9	0.09
B_{2u}	1275.2	0.23	B_{2u}	1275.6	0.11
B_{2u}	1287.2	0.07	B_{1u}	1285.5	1.00
B_{1u}	1333.3	0.06	B_{1u}	1473.3	0.06
B_{2u}	1429.9	0.15	B_{1u}	1505.5	0.07
B_{2u}	1457.9	0.06	B_{1u}	1551.6	0.12
B_{1u}	1485.7	0.16	B_{1u}	1601.2	0.24
B_{2u}	1539.4	0.09	B_{1u}	3037.0	0.07
B_{1u}	1558.4	0.07	B_{1u}	3040.8	0.07
B_{2u}	1567.6	0.28	B_{1u}	3054.7	0.18
B_{1u}	1570.2	0.18	B_{1u}	3078.9	0.08
B_{1u}	1606.5	0.06	B_{2u}	3079.1	0.13
B_{2u}	3021.4	0.62			
B_{1u}	3026.3	0.29			
B_{1u}	3029.5	0.39			
B_{1u}	3045.1	0.89			
B_{2u}	3067.9	0.79			
B_{1u}	3068.0	0.43			

Max. absolute int. Neutral - 5.64 Debye^2/AMU-Å^2 (238.32 Km/mole); Cation - 20.20 Debye^2/AMU-Å^2 (853.55 Km/mole)

3 Discussion and astrophysical significance

Observations of AIBs indicate an extensive abundance of PAHs in various astrophysical environments [12]. Therefore, PAHs are assumed to be important

Table 7
Computed IR Frequencies (cm^{-1}) and Relative Intensities for neutral $C_{96}H_{24}$

	Computed Result		Theoretical Result[1]	
	Freq (cm^{-1})	Rel. Int.	Freq (cm^{-1})	Rel. Int.
B_{3u}	569.1	0.05	586	0.05
B_{3u}	807.9	0.24	800	0.09
B_{3u}	921.2	1.00	912	0.41
E_u	1160.9	0.11	1164	0.09
E_u	1260.7	0.09	1274	0.07
E_u	1397.9	0.06	1418	0.03
E_u	1553.8	0.05	1546	0.05
E_u	1576.9	0.13	1596	0.11
E_u	3020.8	0.61		
E_u	3038.1	0.99	3062	1.00

Max. absolute int. - 7.32 Debye^2/AMU-Å^2 (309.31 Km/mole)
[1] Ref. [26]

inhabitants of the ISM and affect the chemistry of the surroundings. The typical proposed size of these PAHs is likely to be large comprising 50 or more carbon atoms [19–23]. This work is an effort in the direction of providing IR information for larger PAHs. The importance of cation spectra in connection with the astrophysical problem of AIBs has been comprehensively discussed in earlier reports [13,27,28,30–39]. Lack of exact band position match by small PAH cations with the observed AIBs has motivated spectroscopic studies on larger PAHs. The results presented here indicate that the spectra of large PAHs present a better intensity as well as position match with observations.

The Astrophysical infrared emissions depend on the excitation and internal conversion mechanisms in possible PAHs and result from transitions in higher vibrational levels. This may cause the emission features to be broader and slightly red shifted with respect to laboratory absorption bands. The expected shift between emission and absorption is $\sim$10 cm^{-1} which is less than the FWHM considered for plotting the spectra [13]. This red shift may vary with the vibrational mode, PAH size and temperature [55,56]. Moreover, no drastic changes between emission and absorption bands are observed in the few laboratory emission studies available [38,39]. This redshift becomes relevant when spectra of specific astrophysical object is to be modeled using co-added spectra of possible PAHs.

The 3.3 μm (3030 cm^{-1}) feature in large PAHs is generally the most prominent feature of the neutral spectra even if intensity overestimation of $\sim$1.5 times,

Table 8
Computed IR Frequencies (cm^{-1}) and Relative Intensities for $C_{96}H_{24}$ cation

	Computed Result		Theoretical Result[1]	
	Freq (cm^{-1})	Rel. Int.	Freq (cm^{-1})	Rel. Int.
B_{3u}	813.9	0.07	806	0.05
B_{3u}	933.4	0.24	924	0.18
B_{1u}	1163.7	0.06		
B_{2u}	1203.9	0.69	1190	0.49
B_{1u}	1221.9	0.06		
B_{1u}	1223.7	0.15		
B_{1u}	1272.6	0.40	1286	0.33
B_{2u}	1302.6	0.15		
B_{2u}	1302.7	0.19		
B_{2u}	1316.5	0.49	1322	0.69
B_{1u}	1358.8	0.10		
B_{2u}	1426.9	0.06		
B_{1u}	1461.7	0.06	1464	0.36
B_{2u}	1519.6	0.73		
B_{1u}	1540.2	0.41		
B_{2u}	1546.9	0.08		
B_{1u}	1559.4	1.00	1576	1.00
B_{1u}	1569.2	0.12		
B_{2u}	1585.8	0.08		
B_{1u}	1589.0	0.19		
B_{1u}	3062.2	0.09		
B_{1u}	3078.8	0.10		
B_{2u}	3082.7	0.19	3072	0.30

Max. absolute int. - 27.55 Debye^2/AMU-Å^2 (1164.13 Km/mole)
[1] Ref. [26]

due to the use of 4-31G basis for calculation, is taken into consideration. This feature lies in the range 3050 cm^{-1} to 3080 cm^{-1} except for $C_{66}H_{20}$, $C_{90}H_{24}$ and $C_{96}H_{24}$ where it lies near 3030 cm^{-1} presenting a better position match with observations. Upon ionization, this $C-H$ stretch feature is blue-shifted by about 12 to 18 cm^{-1} for all PAHs except for $C_{57}H_{19}$ and $C_{96}H_{24}$ cations where the shift is 43 and 47 cm^{-1} respectively. In cations the $C-H$ stretch intensity is reduced drastically but a gradual increase with size of PAHs is present and a more neutral like intensity is reached in very large species [26,54].

Table 9
Computed IR Frequencies (cm^{-1}) and Relative Intensities for $C_{57}H_{19}$

Neutral		Cation	
Freq (cm^{-1})	Rel. Int.	Freq (cm^{-1})	Rel. Int.
565.6	0.06	842.6	0.13
574.4	0.07	850.6	0.18
795.1	0.07	908.1	0.09
818.2	0.15	934.7	0.21
832.3	0.25	1145.3	0.06
833.1	0.51	1186.2	0.10
890.9	0.24	1188.2	0.11
893.6	0.29	1195.2	0.32
901.3	1.00	1197.9	0.21
1141.7	0.08	1216.8	0.33
1237.4	0.12	1223.2	0.14
1275.4	0.09	1242.7	0.13
1281.4	0.08	1257.7	0.08
1304.4	0.09	1278.8	0.09
1496.5	0.06	1296.1	0.46
1590.9	0.14	1309.8	0.41
1593.8	0.09	1316.8	0.30
1597.2	0.13	1318.5	0.31
1608.1	0.07	1333.4	0.19
3023.0	0.27	1347.5	0.11
3025.4	0.33	1472.1	0.13
3032.4	0.19	1497.4	0.17
3041.7	0.59	1524.5	0.07
3044.1	0.91	1536.6	0.12
3055.4	0.33	1548.5	0.10
3064.7	0.49	1564.3	0.82
3071.3	0.34	1569.3	1.00
3073.2	0.79	1578.4	0.09
3073.5	0.92	1582.8	0.13
3100.2	0.41	1599.3	0.09
		1606.7	0.06
		3057.2	0.09
		3084.4	0.09
		3087.1	0.12

Max. absolute int. Neutral - 2.43 Debye^2/AMU-Å^2 (102.68 Km/mole); Cation - 9.36 Debye^2/AMU-Å^2 (395.51 Km/mole)

The suppression of $C-H$ stretch intensity in PAH cations has been attributed to the partial charge on the hydrogen atoms. With the increase in positive charge on hydrogens there is decrease in the $C-H$ stretch intensity [27,28]. As the PAH size increases the additional charge is distributed over larger number of atoms so the net charge on the hydrogen atoms in large PAH cations is closer to their neutral counterparts. In all the neutral PAHs, including the large PAHs reported here and the sample of catacondensed [27] and pericondensed PAHs [28], the partial charge on hydrogen atoms is 0.13 (in terms of electron charge). For small catacondensed PAH cations, the increased hydrogen charge is 0.18 to 0.20 [27]. Small and medium sized pericondensed PAH cations show a charge of 0.17 to 0.19 on the hydrogens [28]. The charge on hydrogens for large PAH cations ranges from 0.15 to 0.17. The hydrogen charge decreases with increasing size of PAH cations and the corresponding $C-H$ stretch mode intensity increases. PAH anions have even larger $C-H$ stretch intensity (compared to neutral PAHs) as the hydrogen atom charge is lesser than neutrals [25,28]. The effect of ionization on $C-H$ stretch intensity is same for all types of PAHs independent of shape and size.

The $C-H$ out-of-plane bend vibrations are one of the important modes in planar PAH molecules. They give rise to features at 11.2 μm (890 cm^{-1}), 12.7 μm (785 cm^{-1}) and at higher wavelengths depending on the number of hydrogen atoms, their positions and PAH ring structures [53,57]. The observed AIBs have a strong emission band at 11.2 μm with sub features at 12.7 μm, 13.3 μm (750 cm^{-1}) and an underlying plateau. The 11.2 μm feature comes from the out of plane vibrations of solo hydrogen atoms while 12.7 μm from trio hydrogen atoms. In small sized PAHs, the intensity of 12.7 μm band is much larger than that of 11.2 μm feature [27]. Small PAHs have more corners than straight edges, thus, the number of duo and trio hydrogens exceed the number of solos. Large PAHs show a strong 11.2 μm feature [58]. The out-of-plane bend vibrations of solo hydrogens produce intense bands for the currently chosen sample of large PAHs. An exception to this is the spectra of $C_{62}H_{20}$ and its cation. The peripheral structure of $C_{62}H_{20}$ is such that the number of duo hydrogens (eight pairs) exceeds the number of solo hydrogen atoms (four in number). The peak near 844 cm^{-1} (11.85 μm) due to out-of-plane vibrations of duo hydrogens is therefore of higher intensity than the wag of solo hydrogen atoms. For all other large PAHs the solo hydrogen wag feature dominates the 11 to 15 μm range of the spectra. Further, the 11.2 μm PAH feature blue-shifts with increasing PAH size and upon ionization. The band position of the 11.2 μm PAH feature for the studied PAHs and their cations is given in Table 10. For asymmetric $C_{57}H_{19}$ this feature appears at 901 cm^{-1} (11.09 μm) which is closest, among all the studied large PAHs, to the observed astrophysical band. With increasing PAH size, the band is blue-shifted going up to 921 cm^{-1} (10.86 μm) for $C_{96}H_{24}$. There is additional shift in cations. $C_{90}H_{24}$ cation has this feature around 936 cm^{-1} (10.68 μm).

Table 10
Band position of the solo hydrogen wag (11.2 μm AIB) for the studied PAHs and their cations.[1]

PAHs	Neutrals	Cations
$C_{38}H_{16}$	907 (11.0 μm)	927 (10.8 μm)
$C_{48}H_{18}$	916 (10.9 μm)	931 (10.7 μm)
$C_{57}H_{19}$	901 (11.1 μm)	935 (10.7 μm)
$C_{62}H_{20}$	913 (10.9 μm)	933 (10.7 μm)
$C_{66}H_{20}$	917 (10.9 μm)	934 (10.7 μm)
$C_{80}H_{22}$	920 (10.8 μm)	934 (10.7 μm)
$C_{90}H_{24}$	920 (10.8 μm)	936 (10.7 μm)
$C_{96}H_{24}$	921 (10.8 μm)	933 (10.7 μm)

[1]Wavenumber are in cm^{-1}.

In several astrophysical objects many features have been observed between 926 and 904 cm^{-1} (10.8 and 11.06 μm) [59–63]. These features appear as a blue wing (or a shoulder) to the strong 11.2 μm band. Features at 10.8 and 11.1 μm observed by Sloan et al. [63] are more pronounced closer to the central source and fading farther away [64]. The intensity of these bands appears to be a function of the proximity of the exciting star thus acting as a tracer of different PAH populations in the vicinity of the source and away from it. The solo hydrogen wag band position in the spectra of large PAHs lies at a lower wavelength compared to the observed 11.2 μm (893 cm^{-1}) AIB. Correlation between observations and the spectra of large PAHs points to the existence of large PAHs or their cations near the central source. Large PAHs are stable enough to survive the harsh conditions near the exciting source and their spectra agrees well with the observations of the higher frequency features beyond 890 cm^{-1}.

The theoretical spectra of large PAHs show a closer match for the 7.7 (1300 cm^{-1}) and 6.2 μm (1610 cm^{-1}) AIBs. Large neutral PAHs have significantly intense peaks closer to 6.2 and 7.7 μm (1300 cm^{-1}) as compared to small PAHs, though the magnitude of the intensity is not enough to match the AIB intensities. The spectra of cations play an important role in this regard. Except for $C_{90}H_{24}$, $C_{62}H_{20}$ and $C_{38}H_{16}$ cations, the PAH feature corresponding to the 6.2 μm AIB dominates the cation spectra of large PAHs. It is noticed that with increasing cation size, the $C-C$ stretch feature near 1570 cm^{-1} shows regular rise in intensity. A blue shift also accompanies this band with increasing cation size. As extra rings are added to PAHs, the inner $C-C$ bonds have tighter vibrations shifting their band position to higher wavenumbers. In linear polyacenes [27] the inner bonds do not contribute to this mode and there is no such blue shift with size. The blue shift in large PAHs is not systematic and even not enough to match the 6.2 μm (1610 cm^{-1}) position of

Table 11
The band position and relative intensity of the feature close to 1590 cm^{-1} (6.29 μm AIB) for the studied PAH cations.[1]

Studied PAHs	Band position	Relative Intensity
$C_{38}H_{16}$	1591.1 (6.28 μm)	0.98
$C_{48}H_{18}$	1597.9 (6.26 μm)	0.44
$C_{57}H_{19}$	1582.8 (6.32 μm)	0.13
$C_{62}H_{20}$	1591.2 (6.28 μm)	0.23
$C_{66}H_{20}$	1597.9 (6.26 μm)	0.13
$C_{80}H_{22}$	1592.2 (6.28 μm)	0.32
$C_{90}H_{24}$	1601.2 (6.25 μm)	0.24
$C_{96}H_{24}$	1589.0 (6.29 μm)	0.19

[1]Wavenumbers are in cm^{-1}.

the observed AIBs. For most of the studied large PAH cations, this band lies near 1570 cm^{-1} which is away from the 6.2 μm (1610 cm^{-1}) AIB.

Apart from this intense feature, few large PAHs have another peak of significant intensity at 1590 cm^{-1} which is close to the observed 6.29 μm 91590 cm^{-1}) AIB in some sources classified as class 'C' feature [7]. The band position and relative intensity of this mode is tabulated in Table 11. This mode arises from the $C-C$ stretch vibrations of the outer $C-C$ bonds with contributions from few inner $C-C$ bonds. The in-plane bend vibrations of duo hydrogens and $C-C$ stretch of the attached carbons contribute significantly towards this mode in all the studied PAHs.

To compare the infrared spectra of small and large PAHs, co-added spectra of PAHs with $<$ 30 carbon atoms and PAHs with $\geq$ 30 carbon atoms are plotted in Fig. 6. Though the relative intensity of cations satisfy the observed intensity of the 6.2 μm AIB, the band position matching is not good. Failures to explain the position of the 6.2 μm AIB with co-added spectra of pure PAHs calls for studies on PAH clusters and substituted PAHs. Recent calculations on nitrogen substituted large PAH cations (PANHs) [65,66] show that incorporation of nitrogen deep inside the ring, i.e., replacing one or more carbon atoms, shifts the band closer to the AIB feature from 6.4 μm to 6.2 μm.

The 1300 cm^{-1} (7.7 μm) PAH feature in the spectra of large PAH cations present excellent position match and intensity correlation with the observations. The co-added spectra of a composition of medium and small ($\leq$ 32 C atoms) pericondensed PAH cations (Fig. 9 in [28]) shows good agreement with the A' profile of NGC 2023 [7]. The profile variations associated with this band correlate well with the theoretically calculated spectra of large PAH cations as well. The 7.7 μm feature is a composite of two sub-features at 7.6 and 7.8 μm

Table 12
Band positions corresponding to the 7.6 and 7.8 μm AIB of the studied PAHs.[1]

PAHs	7.6 μm AIB	7.8 μm AIB
$C_{38}H_{16}$	1323 (1.24)	1295 (1.19)
$C_{48}H_{18}$		1292 (1.13)
$C_{57}H_{19}$	1312 (1.26)	
$C_{62}H_{20}$	1328 (0.49)	1285 (1.09)
$C_{66}H_{20}$	1304 (0.74)	
$C_{80}H_{22}$		1288 (0.64)
$C_{90}H_{24}$		1284 (1.19)
$C_{96}H_{24}$	1311 (0.77)	1274 (0.47)

[1]Wavenumbers are in cm^{-1} and relative intensities are given in parentheses.

as indicated by observations [7,8,67–69]. Detailed analysis of the theoretical spectra of large PAHs strengthens this proposal. Two sub-components of the 7.7 μm feature for most of the studied large PAHs have been identified and their separation is observed to be similar. The two peaks mainly lie around 1285 cm^{-1} (7.78 μm) and 1315 cm^{-1} (7.60 μm) as presented in Table 12. The intensity of the lower wavelength peak at 1315 cm^{-1} dominates the spectra of $C_{38}H_{16}$, $C_{57}H_{19}$, $C_{66}H_{20}$ and $C_{96}H_{24}$ cations. The 1285 cm^{-1} peak is more intense in the cation spectra of the rest of the studied molecules.

The co-added spectra of large and small PAHs (Fig. 6) show the following distinctive features:

- The $C-H$ stretch has significant intensity in the spectra of cations of large PAHs.
- The intensity of features due to the out-of-plane vibrations of hydrogen atoms has significant differences. The 11.2 μm band is much more intense in the spectra of large PAHs than in smaller ones while the 12.7 μm feature of small PAHs is more intense.
- The 6.2 μm feature has significantly higher intensity for large PAHs both in the neutral and cationic states. This feature is blue-shifted in large PAH cations compared to the small ones but the position fails to match the astrophysical 6.2 μm band.
- The 7.7 μm peak is seen to be arising out of two very close peaks in both the cation spectra (Fig. 6 b).

The above comparison strengthens the role of large PAHs in the context to the mid-IR emission bands. The significance of large PAHs is not only portrayed by its stability but also by its better correlation with the AIBs. This enhances the possibility of large PAHs in different interstellar environments. More studies especially gas-phase IR measurements of large PAHs are needed to put further convincing constraints on interstellar PAHs. The results presented here may

also be used to devise emission models [40–43] for accurate correlation with the AIBs.

4 Conclusion

Results from observations conclude that the 6.2 and 7.7 μm features are the most intense of the interstellar bands and this clearly points toward more ionized PAHs in the ISM. On the other hand, the 3.3 and 11.2 μm bands are a characteristic of neutral PAHs. Hence, both neutral and ionized PAHs contribute towards the interstellar mid-IR spectrum.

Theoretical IR spectra of a few large PAHs are presented in this report. It is noted that the spectra of large PAHs match very well with observed features present on the shorter wavelength side of the strong 11.2 μm band. Small PAHs do not correlate well with the observed intensity and band profiles of these bands. The 11.0 μm blue-wing to the main feature may be attributed to the out-of-plane vibrations of solo hydrogen atoms of large PAHs and their cations. The underlying plateau stretching from 11 to 13 μm points to the contribution from PAH clusters.

The intensity of $C-H$ stretch mode near 3.3 μm in large PAHs is very high. To study relative intensity correlation with other AIBs intensity correction due to overestimation while using 4-31G basis is essential. In the absence of experimental data the correction for the intensity overestimation is not possible. Even if intensity is scaled down by $\sim$1.5 times corelation with observations is not good. Small PAHs show a better correlation with this AIB.

The mode corresponding to 6.2 μm AIB blue-shifts with increasing size of PAH cations. But the shift is not sufficient, even in very large PAHs, to explain the position of the observed 6.2 μm band. Theoretical study of much larger (having more than 100 carbons) and less symmetric PAHs may provide better clues to this problem. PAH clusters and substituted PAHs may also contribute towards this band. Recent studies suggest that incorporation of nitrogen in PAH structures provide a better band position match [65,66].

Observational reports show that the 7.7 μm feature is not a single peak but is a combination of two different peaks at 7.6 and 7.8 μm. Presence of the two sub-components of the broad 7.7 μm feature in large PAHs has been identified. A good profile match with the observations also strengthens the proposition that large PAHs are more feasible to be present in the ISM.

The data presented here enriches the IR information of PAHs. This information may be used for modeling and detailed study of profile variations

accompanying the AIBs in various astrophysical environments. This can lead to a better perception understanding of the PAH chemistry in the ISM and will provide a better knowledge of the associated source.

Acknowledgments

The authors acknowledge the use of High Performance Computing (HPC) and library facilities at Inter University Center for Astronomy and Astrophysics, Pune. AP acknowledges receipt of fellowship from University Grants Commission, New Delhi.

References

[1] F.C. Gillett, W.J. Forrest, K.M. Merrill, Astrophys. J. 183 (1973) 87.

[2] M. Cohen, A.G.G.M. Tielens, J.D. Bregman, F.C. Witteborn, D.M. Rank, L.J. Allamandola, D. Wooden, M. de Muizon, Astrophys. J. 341 (1989) 246.

[3] First ISO Results, Astron. Astrophys. 315 (1996) L26-L400.

[4] B.J. Hrivnak, K. Volk, S. Kwok, Astrophys. J. 535 (2000) 275.

[5] K.I. Uchida, K. Sellgren, H.W. Werner, M.L. Hondashalt, Astrophys. J. 530 (2000) 817.

[6] R. Genzel, C.J. Cesarsky, Ann. Rev. Astron. Astrophys. 38 (2000) 761.

[7] E. Peeters, S. Hony, C. Van Kerckhoven, A.G.G.M. Tielens, L.J. Allamandola, D.M. Hudgins, C.W. Bauschlicher, Astron. Astrophys. 390 (2002) 1089.

[8] E. Peeters, L.J. Allamandola, D.M. Hudgins, S. Hony, A.G.G.M. Tielens, in: A.N. Witt, G.C. Clayton, B.T. Draine (Eds.) ASP Conf. Ser. 309, Astrophysics of Dust, San Francisco: ASP, 2004, p. 141.

[9] A. Leger, J.L. Puget, Astron. Astrophys. 137 (1984) L5.

[10] L.J. Allamandola, A.G.G.M. Tielens, J.R. Barker, Astrophys. J. 290 (1985) L25.

[11] J.L. Puget, A. Leger, Ann. Rev. Astron. Astrophys. 27 (1989) 161.

[12] L.J. Allamandola, A.G.G.M. Tielens, J.R. Barker, Astrophys. J. Supp. Ser. 71 (1989) 733.

[13] L.J. Allamandola, D.M. Hudgins, S.A. Sandford, Astrophys. J. 511 (1999) L115.

[14] A. Li, B.T. Draine, Astrophys. J. 572 (2002) L232.

[15] T.L. Smith, G.C. Clayton, L. Valencic, Astron. J. 128 (2004) 357.

[16] A.L. Mattioda, L.J. Allamandola, D.M. Hudgins, Astrophys. J. 629 (2005) 1183.

[17] A.L. Mattioda, L.J. Allamandola, D.M. Hudgins, Astrophys. J. 629 (2005) 1188.

[18] K. Uchida, K. Sellgren, M.W. Werner, Astrophys. J. 493 (1998) L109.

[19] D.M. Hudgins, L.J. Allamandola, Astrophys. J. 513 (1999) L69.

[20] W.A. Schutte, A.G.G.M. Tielens, L.J. Allamandola, Astrophys. J. 415 (1993) 397.

[21] T. Allain, S. Leach, F. Sedlmayr, Astron. Astrophys., 305 (1996a) 602.

[22] T. Allain, S. Leach, F. Sedlmayr, Astron. Astrophys. 305 (1996b) 616.

[23] V. Le Page, T.P. Snow, V.M. Bierbaum, Astrophys. J. 584 (2003) 316.

[24] S.R. Langhoff, J. Phys. Chem., 100 (1996) 2819.

[25] C.W. Bauschlicher Jr, E.L.O. Bakes, Chem. Phys. 262 (2000) 285.

[26] C.W. Bauschlicher, Astrophys. J. 564 (2002) 782.

[27] A. Pathak, S. Rastogi, Chem. Phys. 313 (2005) 133.

[28] A. Pathak, S. Rastogi, Chem. Phys. 326 (2006) 315.

[29] C.W. Bauschlicher, S.R. Langhoff, Spectrochim. Acta A 53 (1997) 1225.

[30] J. Szczepanski, M. Vala, Nature 363 (1993) 699.

[31] J. Szczepanski, C. Chapo, M. Vala, Chem. Phys. Lett. 205 (1993) 434.

[32] J. Szczepanski, C. Wehlburg, M. Vala, Chem. Phys. Lett. 232 (1995) 221.

[33] D.M. Hudgins, S.A. Sandford, L.J. Allamandola, J. Phys. Chem. 98 (1994) 4243.

[34] D.M. Hudgins, L.J. Allamandola, J. Phys. Chem. 99 (1995) 3033.

[35] D.M. Hudgins, L.J. Allamandola, J. Phys. Chem. 99 (1995) 8978.

[36] D.M. Hudgins, S.A. Sandford, J. Phys. Chem. A 102 (1998) 394.

[37] D.J. Cook, S. Schlemmer, N. Balucani, D.R. Wagner, B. Stelner, R.J. Saykally, Nature 380 (1996) 227.

[38] H.S. Kim, D.R. Wagner, R.J. Saykally, Phys. Rev. Lett. 86 (2001) 5691.

[39] H.S. Kim, R.J. Saykally, Astrophys. J. Supp. Ser. 143 (2002) 455.

[40] E.L.O. Bakes, A.G.G.M. Tielens, C.W. Bauschlicher, Astrophys. J. 556 (2001) 501.

[41] E.L.O. Bakes, A.G.G.M. Tielens, C.W. Bauschlicher, D.M. Hudgins, L.J. Allamandola, Astrophys. J. 560 (2001) 261.

[42] C. Pech, C. Joblin, P. Boissel, Astron. Astrophys. 388 (2002) 639.

[43] C. Joblin, D. Toublanc, P. Boissel, A.G.G.M. Tielens, Mol. Phys. 100 (2002) 3595.

[44] G. Mulas, G. Malocci, C. Joblin, D. Toublanc, Astron. Astrophys. 446 (2006) 537.

[45] GAMESS, M.W. Schmidt, K.K. Baldridge, J.A. Boatz, S.T. Elbert, M.S. Gordon, J.H. Jensen, S. Koseki, N. Matsunaga, K.A. Nguyen, S.J. Su, T.L. Windus, M. Dupuis, J.A. Montgomery, J. Comput. Chem. 14 (1993) 1347.

[46] J. M. L. Martin, J. El-Yazal, and J.P. Francois, J. Phys. Chem. 100 (1996) 15358.

[47] H. Yoshida, A. Ehara, H. Matsuura, Chem. Phys. Lett. 325 (2000) 477.

[48] J.L. Weisman, A. Mattioda, T.J. Lee, D.M. Hudgins, L.J. Allamandola, C.W. Bauschlicher, M.H. Gordon, Phys. Chem. Chem. Phys. 7 (2005) 109.

[49] D.J. De Frees, M.D. MIller, D. Talbi, F. Pauzat, Y. Ellinger, Astrophys. J. 408 (1993) 530.

[50] C.W. Bauschlicher, D.M. Hudgins, L.J. Allamandola, Theor. Chem. Acc. 103 (1999) 154.

[51] G. Herzberg, Molecular Spectra and Molecular Structure, Electronic Spectra and Electronic Structure of Polyatomic Molecules, Van Nostrand, New York, (1966).

[52] M. Breza, Chem. Phys. 291 (2003) 207.

[53] D.M. Hudgins, L.J. Allamandola, Astrophys. J. 516 (1999) L41.

[54] D.M. Hudgins, C.W. Bauschlicher, L.J. Allamandola, Spectrochim. Acta A 57 (2001) 907.

[55] D.J. Cook, R.J. Saykally, Astrophys. J. 493 (1998) 793.

[56] C. Joblin, P. Boissel, A. Leger, L. De'Hendecourt, D. Defourneau, Astron. Astrophys. 299 (1995) 835.

[57] S. Hony, C. van Kerckhoven, E. Peeters, A.G.G.M. Tielens, D.M. Hudgins, L.J. Allamandola, Astron. Astrophys. 370 (2001) 1030.

[58] C. Joblin, L. d'Hendecourt, A. Leger, D. Defourneau, Astron. Astrophys. 281 (1994) 923.

[59] P.F. Roche, D.K. Aitken, C.H. Smith, M.N.R.A.S. 252 (1991) 282.

[60] M.S. Hanner, T.Y. Brooke, A.T. Tokunaga, Astrophys. J. 433 (1994) L97.

[61] M.S. Hanner, T.Y. Brooke, A.T. Tokunaga, Astrophys. J. 438 (1995) 250.

[62] P.R. Roelfsema, et al., Astron. Astrophys. 315 (1996) L289.

[63] G.C. Sloan, T.L. Hayward, L.J. Allamandola, J.D. Bregman, B. DeVito, D.M. Hudgins, Astrophys. J. 513 (1999) L65.

[64] B. DeVito, T.L. Hayward, Astrophys. J. 504 (1998) 43.

[65] D.M. Hudgins, L.J. Allamandola, in: A.N. Witt, G.C. Clayton, B.T. Draine (Eds.) ASP Conf. Ser., Astrophysics of Dust, (San Francisco: ASP) 309 (2003) p. 665.

[66] D.M. Hudgins, C.W. Bauschlicher, L.J. Allamandola, Astrophys. J. 632 (2005) 316.

[67] J.D. Bregaman, L.J. Allamandola, F.C. Witteborn, A.G.G.M. Tielens, T.R. Geballe, Astrophys. J. 344 (1989) 791.

[68] J. Bregman, P. Temi, Astrophys. J. 621 (2005) 831.

[69] G.C. Sloan, L.D. Keller, W.J. Forrest, E. Leibensperger, B. Sargent, A. Li, J. Najita, et al., Astrophys. J. 632 (2005) 956.

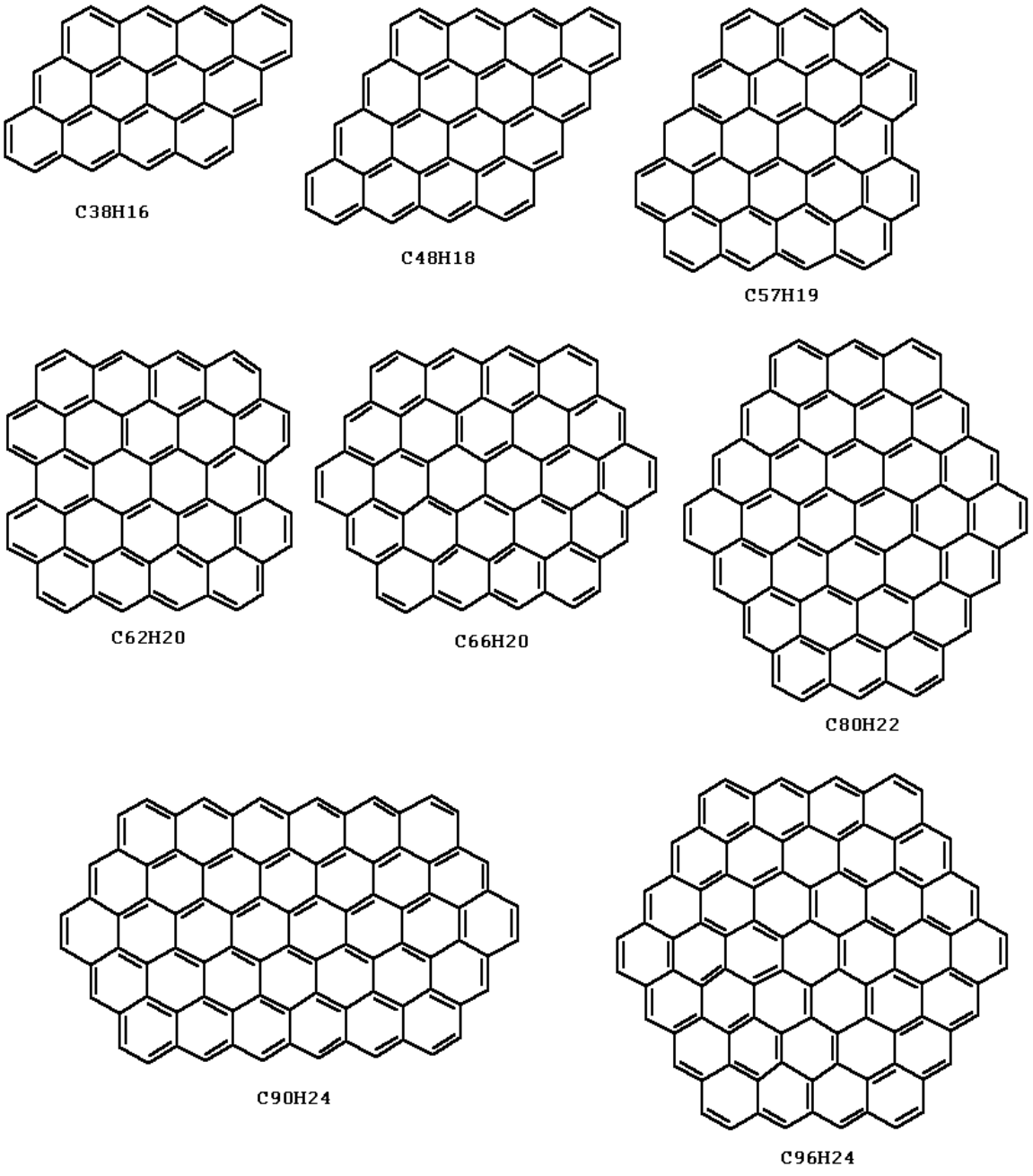

Fig. 1. Studied large PAHs.

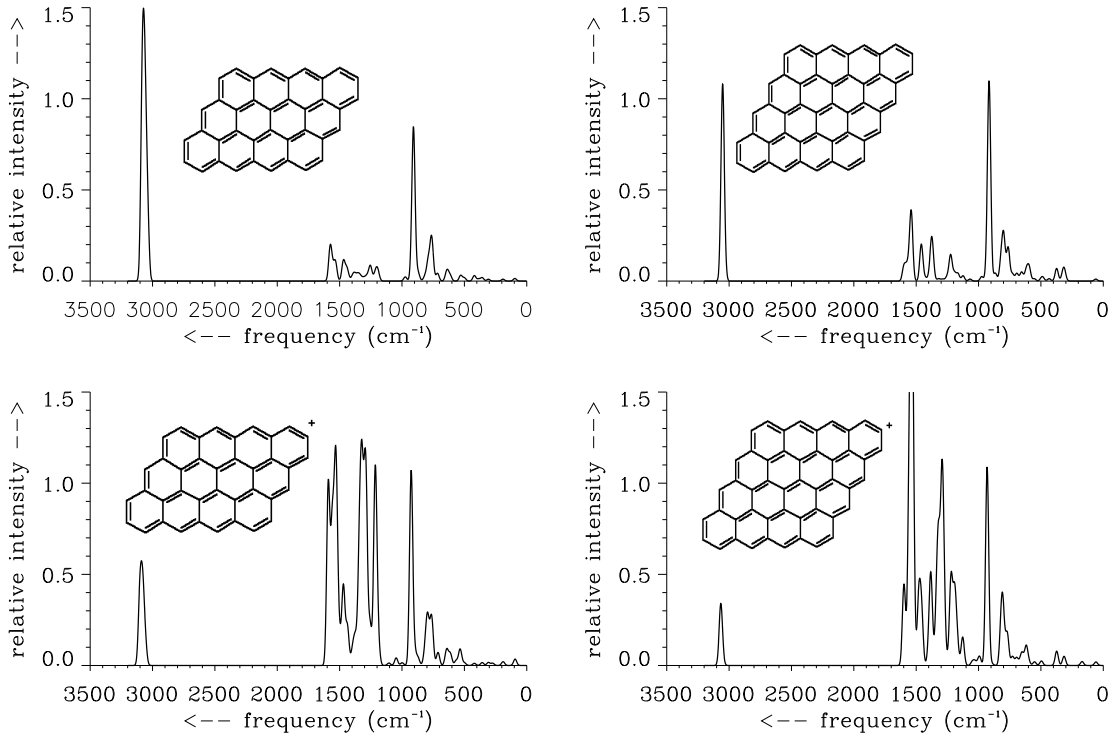

Fig. 2. Infrared spectra of $C_{38}H_{16}$ and $C_{48}H_{18}$.

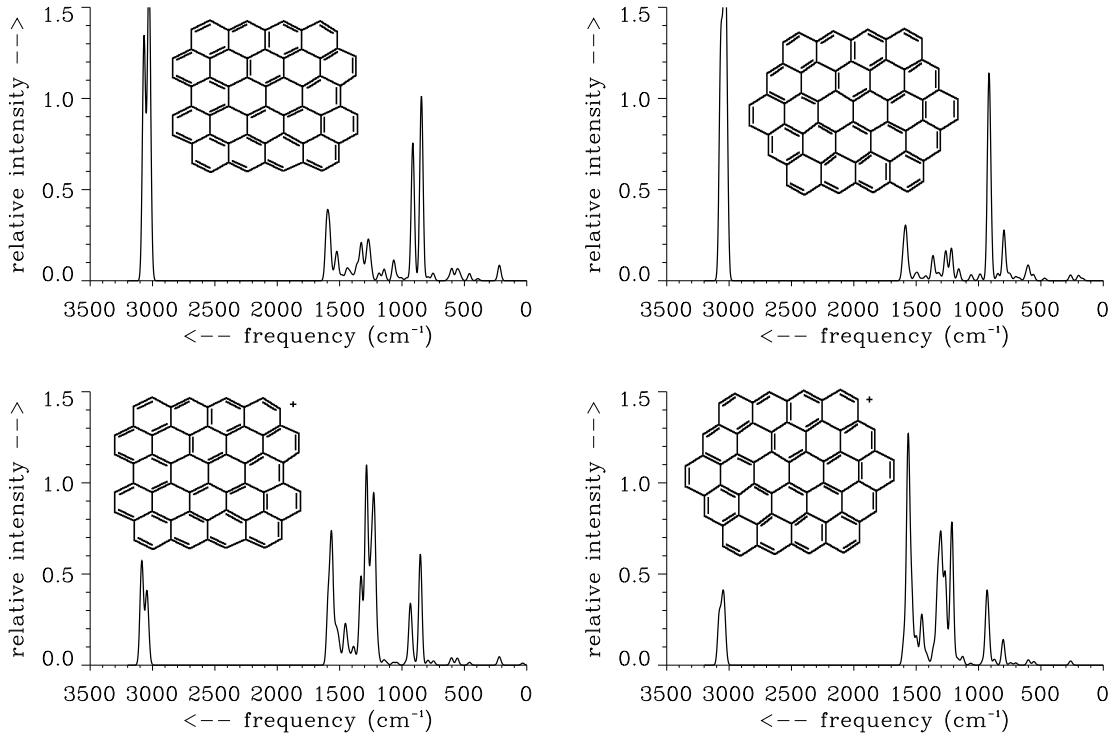

Fig. 3. Infrared spectra of $C_{62}H_{20}$ and $C_{66}H_{20}$.

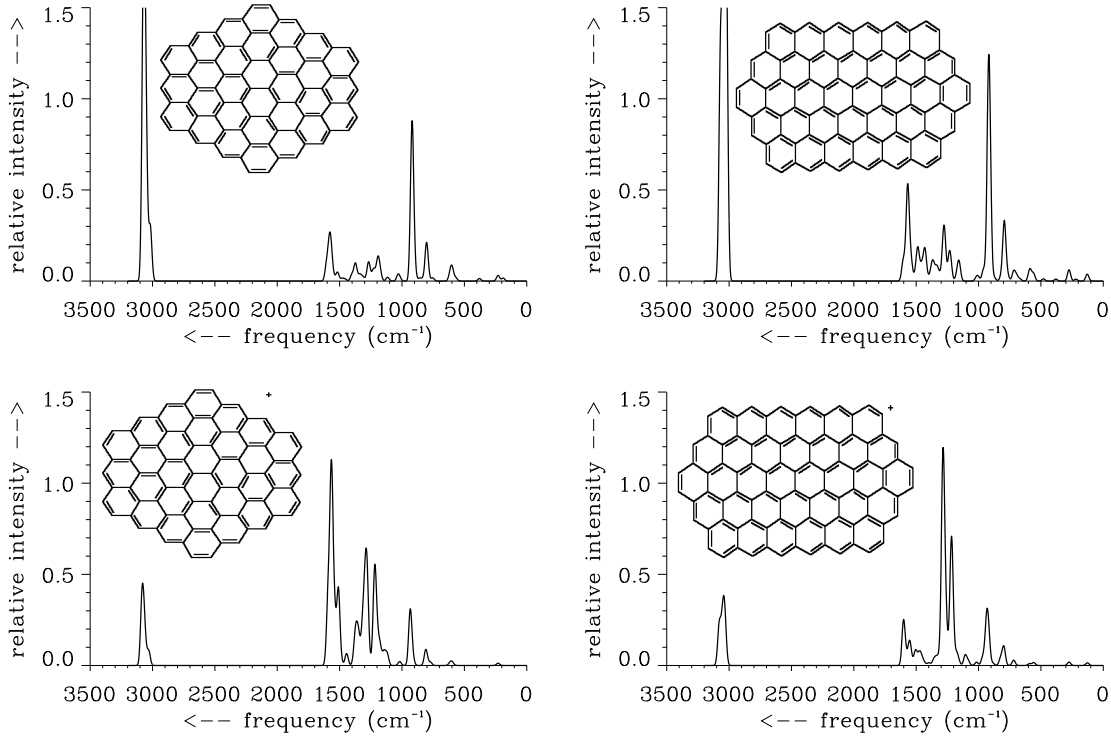

Fig. 4. Infrared spectra of $C_{80}H_{22}$ and $C_{90}H_{24}$.

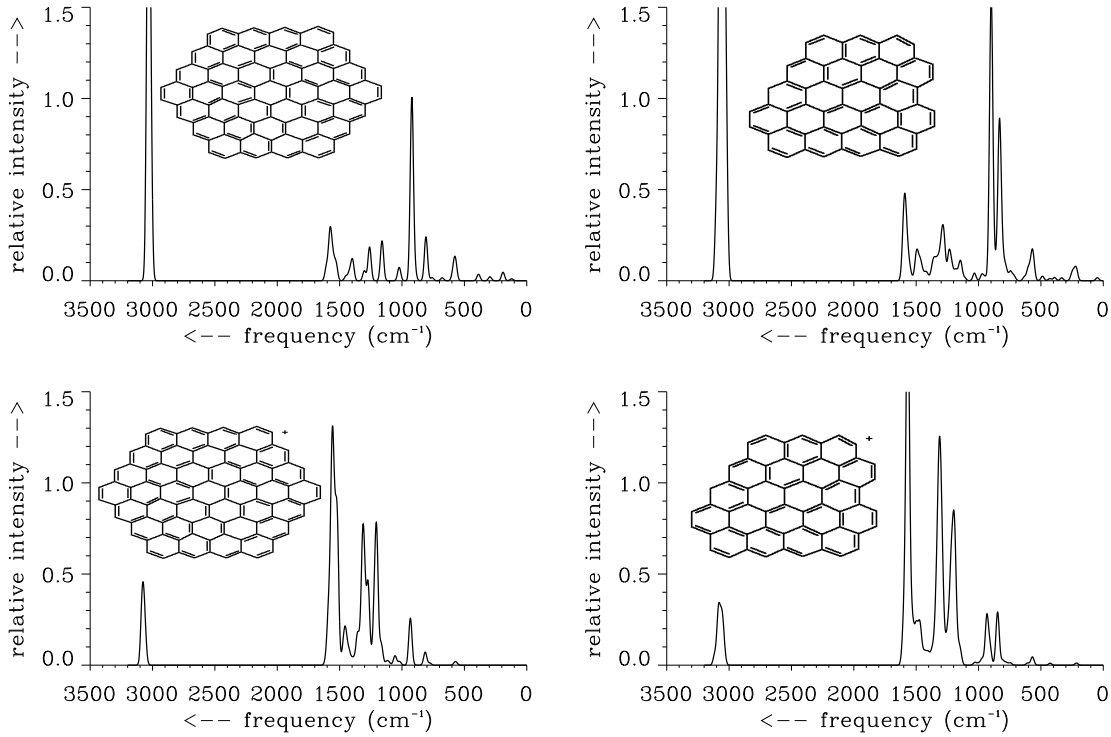

Fig. 5. Infrared spectra of $C_{96}H_{24}$ and $C_{57}H_{19}$.

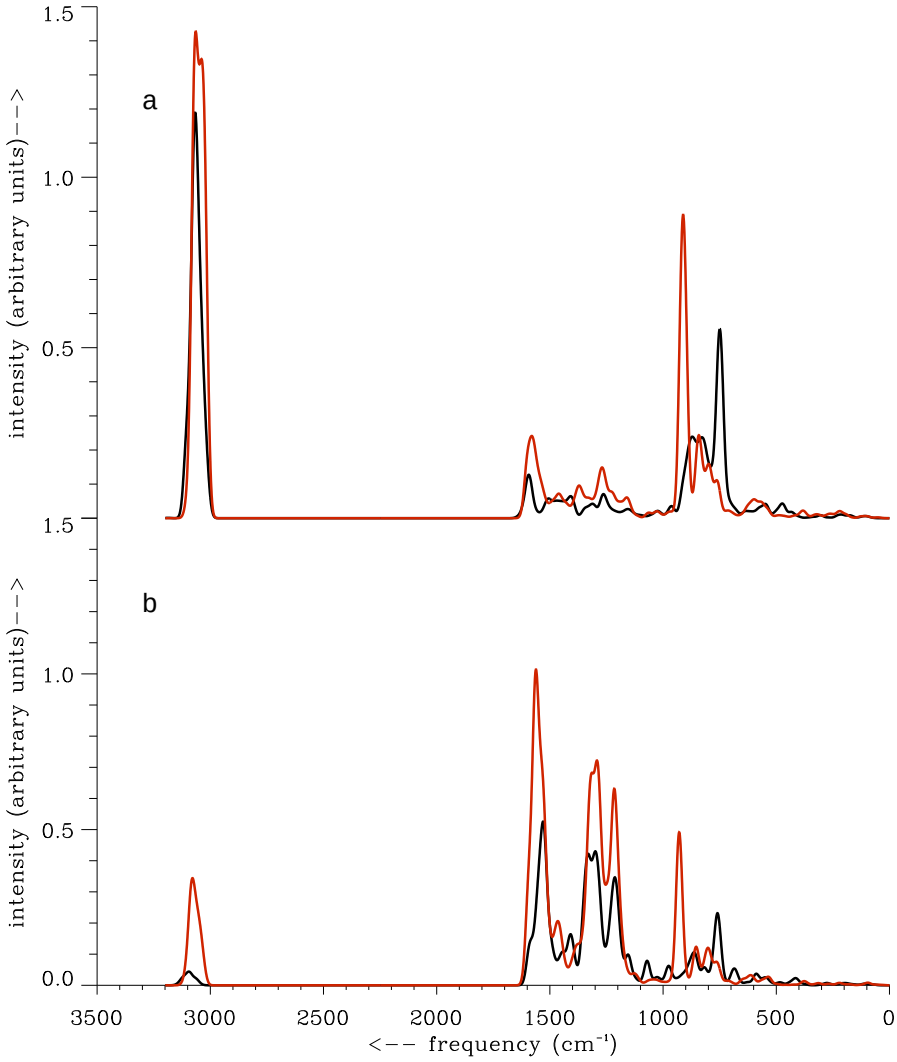

Fig. 6. Comparative co-added spectra of (a) neutral PAHs and (b) PAH cations having less than 30 C atoms (black) and more than 30 C atoms (red).